Published in final edited form as:
Cell Host Microbe. 2014 January 15; 15(1): 58–71. doi:10.1016/j.chom.2013.12.001.

Gut Microbiota of the Tick Vector *Ixodes scapularis* Modulate Colonization of the Lyme Disease Spirochete

Sukanya Narasimhan[1,¶], **Nallakkandi Rajeevan**[2,*], **Lei Liu**[1,*], **Yang O. Zhao**[1,*], **Julia Heisig**[1], **Jingyi Pan**[1], **Rebecca Eppler-Epstein**[1], **Kathleen DePonte**[1], **Durland Fish**[3], and **Erol Fikrig**[1,4,¶]

[1]Section of Infectious Diseases, Department of Internal Medicine, Yale University School of Medicine, New Haven, Connecticut 06520

[2]Yale Center for Medical Informatics, Yale University School of Medicine, New Haven, Connecticut 06520

[3]School of Epidemiology and Public Health, Yale University, New Haven, Connecticut 06520

[4]the Howard Hughes Medical Institute, Chevy Chase Maryland 20815

SUMMARY

Arthopods, such as Ixodes ticks, serve as vectors for many human pathogens. The arthropod gut presents a pivotal microbial entry point and determines pathogen colonization and survival. We show that the gut microbiota of *Ixodes scapularis*, a major vector of the Lyme disease spirochete *Borrelia burgdorferi*, influence spirochete colonization of ticks. Perturbing the gut microbiota of larval ticks reduced *Borrelia* colonization, with dysbiosed larvae displaying decreased expression of the transcription factor STAT. Diminished STAT expression corresponded to lower expression of peritrophin, a key glycoprotein scaffold of the glycan-rich mucus-like peritrophic matrix (PM) that separates the gut lumen from the epithelium. The integrity of the *I. scapularis* PM was essential for *B. burgdorferi* to efficiently colonize the gut epithelium. These data elucidate a functional link between the gut microbiota, STAT-signaling, and pathogen colonization in the context of the gut epithelial barrier of an arthropod vector.

Keywords

Ixodes scapularis; gut microbiota; epithelial barrier; *Borrelia burgdorferi*

[¶]To whom correspondence should be addressed: Sukanya Narasimhan or Erol Fikrig, Section of Infectious Diseases, Department of Internal Medicine, Yale University School of Medicine, S169, 300 Cedar Street, New Haven, CT 06520-8022. sukanya.narasimhan@yale.edu or erol.fikrig@yale.edu.
[*]These authors contributed equally to the described work

SUPPLEMETAL INFORMATION
Supplemental information includes three figures, figure legends, one table listing primer sequences for genes specific to this study, experimental procedures (including 454 pyrosequencing of DNA from larvae and nymphal guts, 16S amplicon sequence analysis, field-collection of nymphal ticks, RNA isolation, quantitative PCR and RT-PCR, RNA interference and immunofluorescence microscopy), and supplemental references relevant to the manuscript. Composition of the microbiota of unfed and fed lab-reared larvae, and unfed nymphs, and field-collected unfed nymphs is archived at http://ngs.med.yale.edu/microbes.

INTRODUCTION

The consortia of microbiota that inhabit the metazoan gut are now recognized as an "organ"-indispensable to host health (Gravitz, 2012; Ley et al., 2008; Spor et al., 2011), and the interactions between commensal bacteria and the vertebrate gut shown to modulate disease outcomes in multiple infectious, metabolic and inflammatory disease models (Clemente et al., 2012). Arthropods vector human and livestock pathogens of immense public health burden world-wide, and are predominantly obligate blood feeders, transmitting and acquiring pathogens during blood feeding (Beaty and Marquardt, 1996; Goddard, 2000). The arthropod gut therefore presents a pivotal microbial entry point that determines the success of pathogen survival, colonization or infection of the vector. Recent studies demonstrate that diverse bacteria inhabit the arthropod gut (Andreotti et al., 2011; Boissiere et al., 2012; Broderick and Lemaitre, 2012; Martin and Schmidtmann, 1998; Rani et al., 2009; Wang et al., 2011), and that these bacteria might be essential players in shaping the vector's stand-off with infectious agents (Cirimotich et al., 2011; Weiss and Aksoy, 2011). Understanding the gut microbiota of arthropod vectors in the context of the pathogens they acquire and transmit may reveal new paradigms to control and prevent vector-borne diseases.

In this study, we examine the gut microbiota of *Ixodes scapularis*, the tick vector of *Borrelia burgdorferi*, the agent of Lyme disease in the North America (Steere et al., 1977). The spirochete is maintained in nature within the black-legged tick, *I. scapularis*, and small mammalian hosts such as *Peromyscus leucopus*, the white-footed mouse (Barbour and Fish, 1993). When *I. scapularis* larvae feed on infected mice, *Borrelia* enter the gut along with the bloodmeal, and colonize the gut via protein-protein interactions (Neelakanta et al., 2007; Pal et al., 2004), and infected larvae then molt to become infected nymphs. When a *B. burgdorferi*-infected nymph feeds on naïve mice, the spirochete replicates, and migrates from the gut to the salivary glands and is transmitted to the host along with tick saliva (Radolf et al., 2012). *Borrelia* acquisition by larval ticks, and *Borrelia* transmission by nymphal ticks thus involves intimate interactions of the spirochete with the gut. In this study, we examine the role of gut microbiota of *I. scapularis* in the context of *Borrelia* acquisition. We describe the diversity of the bacterial species in the *I. scapularis* larval gut by deep pyrosequencing of 16S ribosomal DNA (rDNA) genes and demonstrate that perturbing the composition of the gut microbiota impairs the ability of *B. burgdorferi* to colonize the gut. We suggest that the tick gut microbiota modulate the expression levels of the transcription factor STAT (signal transducer and activator of transcription), the cytosolic component of the JAK (Janus kinase)/STAT pathway (Agaisse and Perrimon, 2004). Activated STAT is known to transcriptionally regulate the expression of immune response genes, and genes involved in epithelial repair, and remodeling (Buchon et al., 2009b; Zeidler et al., 2000). We provide evidence that STAT might orchestrate the expression of peritrophin, a core glycoprotein of the peritrophic matrix (PM), and maintain the structural integrity of the acellular glycoprotein-rich layer that straddles the gut lumen and the gut epithelium (Hegedus et al., 2009). The arthropod PM, akin to the vertebrate gut mucosal layer, provides a barrier essential to prevent both pathogens and indigenous gut bacteria, and abrasive food particles from breaching the gut epithelium (Hegedus et al., 2009). Our study presents a non-traditional role for the *I. scapularis* PM, and suggests that the spirochete exploits the *I. scapularis* PM to shield itself from the blood-filled gut lumen. These observations offer insights into the gut microbiota-vector-pathogen interface.

RESULTS

Dysbiosed larvae show decreased *B. burgdorferi* colonization despite increased engorgement

Ixodes scapularis larvae reared in the lab and maintained under normal conditions (normal containers) were compared to that of *I. scapularis* larvae reared and maintained under "sterile" conditions (sterile containers), and henceforth referred to as "dysbiosed" larvae. Quantitative PCR (qPCR) of bacterial 16S rDNA gene showed decreased total bacterial burden in the unfed dysbiosed larvae when compared to that in normal larvae (Fig 1A). The diversity of the bacterial species in the dysbiosed and normal larvae was assessed by pyrosequencing barcoded, amplified bacterial 16S rDNA from unfed normal and dysbiosed larvae. Unfed normal and dysbiosed larvae were predominantly populated with bacteria of the phyla *Proteobacteria*, *Bacteroidetes*, *Actinobacteria*, *Firmicutes* and *Cyanobacteria*. However, the relative abundance of *Proteobacteria* was higher in dysbiosed larvae, and *Bacteroidetes*, *Firmicutes* and *Cyanobacteria* more abundant in normal larvae (Fig 1B). Bacteria of the genera *Rickettsia*, *Thioclava* and *Delftia* were more abundant in the dysbiosed unfed larvae compared to normal larvae and bacteria of the genera *Aquabacterium*, *Brevibacterium* and *Novosphingobium* increased in abundance in normal unfed larvae (Fig 1C). Principal Coordinate Analysis (PCA) of unweighted jack-knifed UniFrac distances of microbial communities showed that the first and second principle coordinates, which explained 12.56 % and 16.07 % of the variance in the data respectively, separated the unfed normal from unfed dysbiosed larval samples suggesting that larvae raised under sterile conditions had a microbial composition distinct from normal larvae (Fig 1D).

Dysbiosed and normal larvae were fed to repletion on pathogen-free or *B. burgdorferi*-infected C3H/HeN mice and the impact of dysbiosis on larval feeding, *B. burgdorferi* colonization, and larval molting assessed. Dysbiosed larvae fed significantly more on pathogen-free C3H mice when compared to normal larvae as seen by increased engorgement weights (Fig 1E), ($P < 0.05$, n = 250 in pools of 5 larvae). Dysbiosed larvae also fed significantly more than normal larvae on *B. burgdorferi*-infected C3H/HeN mice as seen by increased engorgement weights (Fig 1F) ($P < 0.05$, n = 190 in pools of 5 larvae). Despite increased feeding, qPCR evaluation of spirochete burden in dysbiosed larvae showed significantly decreased *Borrelia* colonization (Fig 1G) ($P < 0.05$, n = 250 in pools of 5 larvae). QPCR assessment of bacterial 16S rDNA showed comparable total bacterial burden in fed dysbiosed and normal larvae (Fig 1H) ($P > 0.05$, n = 250 in pools of 5 larvae).

The composition of the bacterial species of fed larvae (50–75 larvae in pools of 5), assessed as described for unfed larvae, showed that *Proteobacteria* remained the predominant phylum, as seen in unfed normal and dysbiosed larvae. *Proteobacteria* were also more abundant in fed dysbiosed larvae compared to fed normal larvae and *Bacteroidetes* and *Firmicutes* were more abundant in fed normal larvae when compared to fed dysbiosed larvae (Fig 1-I). Feeding increased the diversity in the microbial genera of normal and dysbiosed larvae when compared to unfed larvae possibly due to the protein-rich blood meal (Fig 1-J). Bacteria of the genera *Delftia*, *Acidovorax* and *Rickettsia* were increased in fed dysbiosed larvae when compared to fed normal larvae, and bacteria of the genera Comamonas, Chryseobacterium, Lactobacillus and *Paenibacillus* were more abundant in fed normal larvae (Fig 1-J). The relative increase in anaerobic bacteria such as *Chryseobacterium*, *Lactobacillus* and *Paenicbacillus* in fed normal larvae compared to fed dysbiosed larvae might help balance the redox status of the tick gut and additionally influence bacterial homeostasis (Osset et al., 2001a; Osset et al., 2001b; Piuri et al., 1998). *Rickettsial* bacteria are obligate intracellular bacteria and possibly represent tick endosymbionts associated with the tick gut (Munderloh and Kurtti, 1995). Detailed community compositions at the levels of

phylum, family, class and genera of fed and unfed larvae are archived at http://ngs.med.yale.edu/microbes. PCA along the second and third principle coordinates, which explained 20.52 % and 15.32 % of the variance in the data respectively, separated the fed normal from fed dysbiosed larval samples, and suggested that the composition of the dysbiosed larvae were different from that of normal larvae even after feeding (Fig 1K). Fed-dysbiosed larvae also showed increased molting success when compared to normal larvae (Fig 1L) ($P < 0.05$, n = 450–500 in pools of 50).

To rule out the possibility that rearing under sterile conditions might have imposed "undefined" developmental constraints on the larvae, we allowed normal larvae to engorge on gentamicin-treated mice infected with gentamicin-resistant *B. burgdorferi*, Bb914 (Dunham-Ems et al., 2009). Larvae that engorged on gentamicin-treated mice fed significantly more (Fig S1A) ($P < 0.05$, n = 250 in pools of 5) and demonstrated significantly impaired *Borrelia* colonization (Fig S1B) ($P < 0.05$, n = 100 in pools of 5) when compared to larvae that fed on buffer-treated mice.

Expression of signal transducer and activator of transcription (*stat*) is decreased in dysbiosed *I. scapularis* larvae

The phenotypic outcomes of dysbiosis are possibly multifactorial, and we reasoned that increased innate immune responses in the gut of dysbiosed larvae might account, in part, for decreased *Borrelia* colonization. Knowledge of innate immune pathways of *I. scapularis* is still rudimentary (Kopacek et al., 2010). A key signaling pathway implicated in arthropod gut immunity, and homeostasis is the JAK/STAT pathway with its simple yet potent 3-component system that regulates development, wound repair and remodeling, and immunity (Zeidler and Bausek, 2013). Our earlier work has shown that the *I. scapularis* genome encodes a functional Signal Transducer and Activator of Transcription (STAT) (Liu et al., 2012). Although STAT activation is a post-translational event (Agaisse and Perrimon, 2004), expression levels of *stat* are coincident with STAT activity and the concomitant modulation of STAT-regulated genes (Liu et al., 1995). Quantitative reverse transcriptase-PCR (qRT-PCR) analysis of the transcript levels of *stat* showed a significant decrease in the expression levels of *stat* in fed dysbiosed larvae compared to normal larvae (Fig 2A) ($P < 0.05$, n = 50 in pools of 5 larvae). Further, expression of an *I. scapularis* homolog of *Drosophila socs-2* (*ISCW015921*), a negative regulator of the JAK/STAT pathway, and indicator of activation of the JAK/STAT pathway (Karsten et al., 2002), was also decreased in dysbiosed larvae compared to normal larvae (Fig 2B) ($P < 0.05$, n = 50 in pools of 5 larvae) and suggested that dysbiosis might impact signaling via the JAK/STAT pathway.

RNA interference-mediated decrease in *stat* expression in *I. scapularis* nymphs results in decreased *B. burgdorferi* colonization

To examine the role of *stat* in *Borrelia* colonization, we exploited the RNA interference (RNAi) technique (Fire et al., 1998). RNAi has been adapted for nymph and adult stages (Aljamali et al., 2002), but not for the larval stage, due mainly to the small size of the larvae that precludes efficient delivery of ds RNA into larvae, and increases larval mortality from injection trauma. Therefore, we utilized the nymphal stage and knocked down the expression of *stat* to recapitulate the expression profile observed in dysbiosed larvae (Fig 2A). We injected *dsstat* RNA into the anal pore of unfed clean *I. scapularis* nymphs and allowed the ticks to feed to repletion on *B. burgdorferi*-infected C3H/HeN mice. Control nymphs, injected with *dsgfp* RNA, and *dsstat* RNA-injected nymphs had comparable engorgement weights (Fig 2C). Decreased *stat* expression, as measured by qRT-PCR, in the guts of *dsstat* RNA-injected repleted nymphs (Fig 2D) resulted in significantly decreased *B. burgdorferi* burdens when compared to that in control repleted nymphs (Fig 2E) ($P < 0.05$, n = 35–40 nymphs in pools of 2–3 guts), and phenocopied dysbiosed larvae (Fig 1).

Decreased *stat* expression compromised epithelium renewal of the tick gut and altered gut morphology

The JAK/STAT signaling pathway is involved in epithelial remodeling, and regeneration to compensate for wear and tear during feeding and microbe-induced damage (Buchon et al., 2009a). We first examined by immunofluorescence, the levels of mitotic activity as a score of epithelium renewal in the guts of normal nymphal guts by staining for phosphorylated histone 3 (PH3), a marker of mitotic activity (Amcheslavsky et al., 2009). The kinetics of mitotic activity showed peak activity at about 48 h of feeding, with little or no activity at repletion (96 h of feeding) (Fig S2A–B). We then assessed the mitotic activity in the guts of *dsstat* or *dsgfp* RNA-injected nymphs at 24, 48 and 72 h post-attachment. Significantly decreased mitotic activity in the guts of *dsstat* RNA-injected nymphs when compared to that in *dsgfp* RNA-injected nymphs at 72 h of feeding ($P < 0.05$, n = ~10 guts/time point) (Fig 3A–B) suggested that repair and renewal of the *I. scapularis* gut epithelium might be regulated by STAT activity as seen in *Drosophila* (Buchon et al., 2009a). We do not have reagents, at this juncture, to determine whether the PH3-positive cells are tick gut stem cells or digestive epithelial cells.

We then examined the gross morphology of the guts of Carnoy's fixed *dsstat* or *dsgfp* RNA-injected 24 and 72 h fed-nymphs (representing an early- and late-feeding phase) by Periodic acid-Schiffs base stain (PAS) to detect the glycan-rich peritrophic matrix of *I. scapularis*. Interestingly, when *stat* expression was decreased, the glycoprotein rich peritrophic matrix (PM)-like layer, separating the epithelial cells and the gut lumen was also significantly decreased in thickness in *ds stat* RNA-injected nymphs compared to control nymphs (Fig 3C–D) at 24 and 72 h of feeding, coincident with RNAi-mediated *stat* knockdown at 24 h and 72 h of feeding (Fig S2C). However, the phenotypic impact of *stat* knockdown on *Borrelia* colonization was significant only around 72 h of feeding (Fig S2D).

To determine if alterations in the gut microbiota might also influence the structure of the gut barrier, the guts of normal larvae that engorged on gentamicin-treated mice, and dysbiosed larvae that engorged on normal mice were similarly examined by PAS staining. Sectioning of 24 h (guts too small) and 72 h fed /repleted fed larval tick guts (guts too full of blood) was technically challenging, hence, larval guts were examined at 48 h of feeding, and we observed significantly decreased thickness of the PM-like layer in dysbiosed and gentamicin-exposed larval guts when compared to normal or PBS-exposed larval guts (Fig 3E–G).

Decreased *stat* expression was reciprocated by decreased *peritrophin-1* expression

A major glycoprotein of arthropod PM is peritrophin (Lehane, 1997). The genome of *I. scapularis* encodes several putative peritrophins (www.vectorbase.org) with homology to insect peritrophins (Shao et al., 2005). *In silico* assessment of the 5′UTR regions of the putative *I. scapularis peritrophin* genes, ISCW006076, ISCW013030, ISCW007687, ISCW013029, and ISCW024120, henceforth named *peritrophin-1, 2, 3, 4 and 5* respectively showed canonical STAT binding sites, TTCNNNGAA or TTCNNNNGAA (Agaisse and Perrimon, 2004; Rivas et al., 2008) (Fig S3A), suggesting that expression of *I. scapularis peritrophins* might be regulated by STAT. qRT-PCR assessment of the expression levels of the *peritrophins* showed significantly decreased levels of *peritrophin-1*, and *2* in *ds stat* RNA-injected fed nymphs compared to that in control nymphs (Fig 4A–B) ($P < 0.05$, n = 35–40 nymphs in pools of 2 nymphal guts). Importantly, the expression of *peritrophin-1* was also significantly decreased in dysbiosed, and in gentamicin-exposed fed larvae compared to normal fed larvae (Fig 4D and F) ($P < 0.05$, n = ~ 100 larvae in pools of 5). *peritrophin-2* expression levels were not detectable in the larval stage. While expression of *peritrophin-4* was significantly decreased in fed dysbiosed larvae (Fig 4E), the expression was not altered

in *stat*- knockdown nymphal guts (Fig 4C) and in gentamicin-exposed larvae (Fig 4G). Expressions of *peritrophin-3* and 5 were not altered in dysbiosed, and in gentamicin-exposed fed larvae, and in *stat*-knockdown nymphal guts (Fig S3B)

These observations suggested that the expression of *peritrophin-1* was likely modulated by STAT in the larval stage. We examined if STAT might bind to the conserved STAT-binding regions of the *peritrophin-1* promoter (Fig S3A) using the **e**lectrophoretic **m**obility **s**hift **a**ssay (EMSA). Biotinylated oligonucleotide probes containing the conserved STAT binding regions of the *peritrophin-1* promoter (Table S1) were incubated with recombinant tick STAT (Liu et al., 2012) and analyzed by EMSA. Shift in the mobility of the probe DNA suggested that rSTAT bound to the *peritrophin-1* promoter (Fig 4H). Further, this binding could be competed by an excess of unlabeled oligonucleotide probe containing the STAT binding site of *perirophin-1*, but not by an irrelevant oligonucleotide probe (Fig 4H). The binding could not be supershifted by polyclonal anti- rSTAT antibody, possibly because of the inability of the antibody to recognize DNA-bound STAT (data not shown). We then performed RNA-Fluorescence *In Situ* Hybridization (RNA-FISH) to determine if *stat* mRNA was expressed in cells expressing *peritrophin*-1 mRNA. We utilized 48 h fed tick guts, a time point coincident with increased STAT activity (Fig 3), and observed specific staining with Alexa Fluor-labeled antisense RNA probes and co-localization of *stat* and *peritrophin* RNA in the epithelial cells lining the gut lumen (Fig 4I).

RNA interference-mediated decrease in *peritrophin* expression resulted in decreased *B. burgdorferi* colonization

Since *peritrophin-1* appeared to be predominantly expressed in larval and nymphal stages compared to the other peritrophins (Fig 4), we reasoned that *peritrophin-1* might be the major component of the *I. scapularis* PM-like layer. To better understand if STAT-regulated alteration of the *I. scapularis* peritrophic matrix influenced *B. burgdorferi* colonization of the gut, we injected *dsperitrophin-1* RNA into the anal pore of clean *I. scapularis* nymphs and allowed ticks to feed to repletion on *B. burgdorferi*-infected C3H/HeN mice. Nymphs injected with *ds peritrophin-1* RNA or *dsgfp* RNA engorged comparably (Fig 5A). Decreased *peritrophin* expression in *ds peritrophin* RNA-injected nymphs (Fig 5B) resulted in significantly decreased *B. burgdorferi* burden when compared to that in normal larvae (Fig 5C) ($P < 0.05$, n = 25–28 nymphs in pools of 2–3 nymphal guts), phenocopying the *stat* knockdown phenotype (Fig 2). PAS staining of the tick guts showed decreased thickness of the glycosylated PM-like layer at 72 h of feeding (Fig 5D–E), and suggested that decreased expression of *peritrophin-1* compromises the structural integrity of the PM-like barrier matrix.

Integrity of the peritrophic matrix is critical to distance the spirochete from the gut lumen during colonization

Arthropod PM provides a vital permeability barrier-preventing microbes and food /blood meal debri from reaching the gut epithelium (Kuraishi et al., 2011). Compromised permeability barrier therefore presents a likely functional consequence of the thinning of the PM. Since *peritrophin-1* knockdown resulted in PM thinning later in feeding (Fig 5), and presence of a large blood meal confounded visualization of fluorescent dextran, we used stat-knockdown ticks to assess the impact of PM thinning on PM permeability. We introduced a cocktail of Rhodamine-red-conjugated 10,000 MW and Fluorescein-conjugated 500,000 MW dextran into the guts of ds *stat* or ds *gfp* RNA-injected 24 h-fed nymphs by capillary feeding and examined the unfixed guts immediately under a confocal microscope. The 10,000 MW dextran diffused out from the lumen readily and reached the epithelial cells (Fig 6A) in both ds *gfp* and ds *stat*-RNA-injected nymphs. The 500,000 MW dextran was predominantly localized to the gut lumen and undetectable near the epithelial cells of ds gfp-

injected nymphs, but more frequently observed close to the epithelial cells of ds *stat* RNA-injected nymphs (Fig 6A).

Spirochetes adhere to the gut epithelium for successful colonization (Pal et al., 2004). Compromised permeability barrier might expose the epithelium-bound spirochetes to deleterious blood meal components and foil colonization. Immunofluorescence staining of Carnoy's fixed guts of *dsgfp* RNA-injected nymphs fed on *B. burgdorferi*-infected mice showed that *Borrelia* entering into the tick gut adhered predominantly to the gut epithelial cells at 24 and 72 h of feeding (Fig 6B). In contrast, in *dsstat* RNA-injected nymphs, *Borrelia* or *Borrelia* debris was observed in the luminal side of the guts at 24 and 72 h of feeding (Fig 6B) and decreased epithelium-bound spirochetes. RNAi-mediated decrease in the expression of *peritrophin-1* also showed decreased *Borrelia* adherence to the gut epithelial cells, although we could not detect spirochetes in the luminal side (Fig 6B).

Indigenous microbial profile of *I. scapularis* in endemic areas

Relating the microbiota profiles in lab-reared ticks with that observed in ticks in their natural habitats in Lyme disease endemic areas is critical to forge meaningful insights into vector-gut bacteria interactions. Hence, we assessed the composition of the bacterial species in unfed nymphs collected from Branford, CT as described for larvae and compared it to lab reared nymphs and larvae (Supplemental data archived at: http://ngs.med.yale.edu/microbes). Gut microbial composition of field-collected nymphs showed significant similarities with that in lab-reared nymphs both at the phylum and genus levels (Fig 7A–B) with the exception of increased abundance of *Rickettsia* and decreased abundance of *Acidovorax* in lab-reared nymphs compared to field-collected nymphs. Larvae and nymphs showed distinct differences in the microbial compositions at the genera level, but not at the phylum level. PCA showed that the first and third principle coordinates, which explained 15.2 % and 8.4 % of the variance in the data respectively, separated the unfed dysbiosed larval samples from both unfed normal larvae and unfed field nymphs, and clustered the unfed normal larvae relatively closer to unfed field nymphs (Fig 7C). Further, PCA analysis along the second and third principle coordinates, which explained 7.85 % and 7.47 % of the variance in the data respectively, separated unfed nymphs from unfed larvae, but clustered lab-reared unfed nymphs closely with field-collected unfed nymphs (Fig 7D), indicative of a stage and niche-specific association of these bacteria to the tick gut.

DISCUSSION

In this study, we addressed the gut microbiota of *Ixodes scapularis*, and its interplay with the tick vector in the context of *B. burgdorferi* colonization. The diet of *I. scapularis* is strictly limited to vertebrate blood and, presumably, blood from pathogen-free hosts is sterile. It is conceivable that bacteria are acquired from the environment through oral, respiratory, and genital orifices that might allow the tick to sample and engage with environmental microbiota, and some bacteria are possibly transovarially inherited (Munderloh and Kurtti, 1995). Ways to artificially feed *I. scapularis* ticks are not fully optimized (Broadwater et al., 2002), hence, rearing germ-free *I. scapularis* remains technically challenging. To address the potential role of the *I. scapularis* gut bacteria in modulating *B. burgdorferi* colonization, we allowed *I. scapularis* eggs to hatch in containers that were sterile and manipulated in a biosafety hood. While this is not a bona-fide germ-free environment, we reasoned that larvae that hatch in a "sterile" environment would demonstrate an altered microbiota profile when compared to larvae that hatch in a normal environment.

Indeed, 454 FLX-Titanium pyrosequencing (Margulies et al., 2005) of the 16S amplicons revealed distinct differences in the microbial composition of "sterile-container"-raised larvae when compared with that in normal larvae and hence these larvae were referred to as

dysbiosed larvae. Dysbiosed larvae and larvae that fed on gentamicin-treated mice demonstrated significantly increased engorgement weights, and decreased *B. burgdorferi* colonization when compared to normal larvae. Gentamicin entering the gut of normal larvae along with the blood meal expectedly would be detrimental to the normal gut flora of the engorging larvae and result in dysbiosis. Together, these observations suggested a potential role for altered gut microbiota in increased feeding, and impaired *Borrelia* colonization. Prolonged use of gentamicin in mammalian hosts has been shown to cause ototoxicity potentially due to its ability to induce nitric oxide synthase leading to oxidative stress (Hong et al., 2006). Although exposure of tick guts to gentamicin for 3–4 days did not manifest obvious adverse phenotypes, the impact of gentamicin on tick physiology remains to be addressed. Species level identification of the differentially represented bacterial genera in normal and dysbiosed larvae might facilitate functional correlations between specific bacterial species and *Borrelia* colonization. Importantly, the microbial composition of field-collected nymphs was similar to that in lab-reared nymphs raising the possibility that functional insights obtained from lab-reared ticks in the context of tick microbiota-pathogen interactions might be extrapolated to field ticks.

Efforts to determine if increased innate immune responses in the gut of dysbiosed larvae might account, in part, for decreased *Borrelia* colonization revealed decreased expression levels of *stat* in dysbiosed larvae as well as gentamicin-exposed larvae. The JAK/STAT pathway is charged with functions relating to wound repair, remodeling and epithelium renewal in response to tissue damage upon stress and infection (Buchon et al., 2009a). Dysbiosed microbiota might engage in a less “inflammatory” dialogue with the tick gut and consequently trigger the STAT-signaling pathway to a lesser extent. In *Drosophila* decreased STAT activation resulted in increased susceptibility to pathogen infection (Buchon et al., 2009a). In contrast, decreased *stat* resulted in decreased *Borrelia* colonization of the tick gut suggesting that STAT activation-induced gut epithelium renewal that accompanies normal feeding might provide components vital for *Borrelia* colonization of the gut.

PAS stain of *stat*-knockdown nymphal, and dysbiosed and gentamicin-exposed larval guts showed a significant decrease in the glycan-rich layer separating the gut lumen from the gut epithelium. The glycan-rich layer corresponds to the *I. scapularis* peritrophic membrane (PM) (Sojka et al., 2007), and appears to be generated by the midgut cells within 9–12 hours of the onset of feeding (Grigor’eva and Amosova, 2004). A major glycoprotein of arthropod PM is peritrophin (Lehane, 1997). Canonical STAT binding sites (Rivas et al., 2008) in the 5′UTR regions of *I. scapularis peritrophin-1*, in conjunction with *in vitro* demonstration of STAT binding to the promoter region of *peritrophin-1* by EMSA, and RNA-FISH validation of co-expression of *stat* and *peritrophin*-1 transcripts in gut epithelial cells suggested that STAT might modulate the expression of *peritrophin-1*. The decreased expression of *peritrophin*-1 in dysbiosed and gentamicin-exposed larvae suggested a functional link between gut microbiota-*stat* and *peritrophin-1* expression.

Buchon *et al* (Buchon et al., 2009b) showed that in *Drosophila* genes encoding putative peritrophins might be under the control of the IMD pathway that directly senses microbial components of gram-negative bacteria (Welchman et al., 2009). *peritrophin-4* transcripts were decreased in dysbiosed larvae, but not in *stat*-knockdown nymphal guts. Conceivably, an IMD-like pathway might regulate *I. scapularis peritrophin-4*. That the components of the peritrophic matrix might be under the control of multiple gut immune-surveillance pathways is physiologically relevant. Normal gut bacteria engagement with the IMD pathway as well as routine wear and tear induced STAT activation (Buchon et al., 2009b; Jiang et al., 2009) might help fortify the PM.

The low pH (~ 6–6.5) in the tick gut might favor partial release of oxygen, and heme from host hemoglobin in the blood meal, (Jeney et al., 2002), and host cellular components including neutrophils present in the blood meal might present a noxious milieu to the spirochetes. Therefore, it might be imperative for *Borrelia* to distance itself from the gut lumen once it enters the tick vector, and the PM likely provides that opportunity for the spirochete. Our observations suggest that the thinning PM in *stat* knockdown guts leads to increased PM permeability. This might: A. expose epithelium-bound spirochetes to the blood meal pro-oxidants and cellular components detrimental to spirochetes; and B. bring gut bacteria in closer proximity to the gut epithelium, inadvertently elevate gut epithelial immune responses (Kuraishi et al., 2011; Weiss et al., 2013), and further compromise *Borrelia* colonization. In addition to its structural barrier function, peritrophin-like proteins have been invoked in heme detoxification to preempt gut damage (Devenport et al., 2006), and in killing Gram-negative bacteria (Du et al., 2006). If tick peritrophin-1 functions thus, it might additionally influence gut integrity and gut bacterial homeostasis.

Increased engorgement of dysbiosed larvae is likely not STAT-mediated since RNAi-mediated decrease in *stat* levels in the nymphal gut did not alter engorgement weights. Other pathways altered by dysbiosis, or by STAT, in its role as transcription factor (Arbouzova and Zeidler, 2006; Rajan and Perrimon, 2012), may additionally influence *Borrelia* colonization, tick feeding, and molting. Direct competition or dependence for a nutrient-niche between commensal microbiota and pathogens has been invoked in resistance to bacterial colonization of the vertebrate gut (Ng et al., 2013). It is likely that dysbiosis might also pose an unfavorable nutrient-niche for the spirochete.

These findings suggest that the indigenous microbiota of *I. scapularis* maintain a critical cross talk with the tick gut to modulate the structural and functional integrity of the tick gut in favor of *Borrelia* colonization. Hence, specific microbial compositions might be central to vectorial capacity. How tick gut microbiota broker gut barrier responses remains to be addressed and such an understanding might catalyze ways to control vector-borne pathogens.

EXPERIMENTAL PROCEDURES

Generation of dysbiosed *I. scapularis* larvae

About 15 adult *I. scapularis* females fed to repletion on the ears of rabbits (Das et al., 2001), were surface sterilized with 70 % ethanol in a Laminar Flow Biosafety cabinet, placed in sterile/pyrogen-free tubes covered with sterile meshes, and tubes individually placed in polypropylene sterile blue-capped tubes, and transferred to an incubator maintained at 23°C with 85% relative humidity and a 14/10 h light/dark photo period regimen for egg laying and hatching. Larvae that hatched in sterile tubes were designated dysbiosed larvae. Control adults were placed in non-sterile tubes and incubated as described above to obtain normal larvae.

Borrelia burgdorferi N40 or *B. burgdorferi* 914 infection of mice

B. burgdorferi N40 (Thomas et al., 2001) or *B. burgdorferi* 914 (Dunham-Ems et al., 2009) was used to inoculate C3H mice as described before (Narasimhan et al., 2007). Skin punch biopsies were collected from each mouse 2 weeks after inoculation, and tested by QPCR for the presence of spirochetes as described (Narasimhan et al., 2007). Comparably infected mice were utilized in all *B. burgdorferi* acquisition experiments.

Antibiotic treatment of mice

Two weeks after C3H mice were infected with *B. burgdorferi* 914 (Dunham-Ems et al., 2009), 100 μl of gentamicin (Life Technologies, CA) was given at a concentration of 1 mg / 20 Kg body weight of mice intra-peritoneally 24 h prior to placement of larvae, and subsequently once each day intraperitoneally for the next 3–4 days until the larvae had all repleted and detached. Using the same regimen, control animals received 100 μl of PBS/20 Kg body weight of mice.

Sectioning of nymphs and larvae, and staining

Nymphs fed for 24, or 72 h and larvae fed for 48 h were fixed in Carnoy's fixative for 1 hour, washed in graded alcohol followed by 3 washes in Xylene, paraffin embedded and sectioned at 3–5 μm, and sections stained with Periodic acid Schiffs base (PAS) at the Yale Histology Core Facility as described (Hladik, 1997) and visualized under a Zeiss Axio YLCW023212 microscope at 40X magnification using the ZEN Lite software (Carl Zeiss Inc, NY). The thickness of the PAS positive PM-like layer was assessed in 3 different regions in each microscopic field, and arithmetic average computed. At least 3 fields / section was assessed and 6–10 individual sections examined /group. Deparaffinized sections were stained for *B. burgdorferi* using FITC-labeled affinity purified goat anti *B. burgdorferi* antibody (KPL, MD) and nuclei counterstained with TO-PRO-3 (Invitrogen, CA) and visualized at 63x magnification under a Zeiss LSM510 confocal microscope.

Electrophoretic Mobility Shift Assay (EMSA)

EMSA assay to determine STAT binding to the peritrophin-1 promoter region was conducted using the Light Shift Chemiluminescent EMSA kit (ThermoScientific, IL) as directed by the manufacturor. See Supplemental Experimental Procedure for details.

RNA-Fluorescence in situ hybridization (RNA-FISH)

RNA-FISH for the detection of stat and peritrophin-1 transcripts in tick gut epithelim was performed using the FISH Tag™ RNA multicolor kit (Invitrogen, CA) as suggested by the manufacturor. See Supplemental Experimental Procedure for details.

Artificial feeding of nymphs

Nymphs were injected with ds *gfp* or ds *stat* RNA and allowed to feed on naïve pathogen-free mice for 24 h as described above (15–20 nymphal ticks/mouse). The nymphs were removed and capillary fed as described earlier (Soares et al., 2005) with a solution of fluorescein-conjugated dextrans. See Supplemental Experimental Procedure for details.

Statistical analysis

The significance of the difference between the mean values of the groups was analyzed using a non-parametric two-tailed Mann-Whitney test with Prism 5.0 software (GraphPad Software, USA), and $P < 0.05$ was considered significant.

Supplementary Material

Refer to Web version on PubMed Central for supplementary material.

Acknowledgments

We are grateful to Dr. Ruth Ley at Cornell University for guidance with the 16S amplicon library preparation, Dr. Justin Radolf at the University of Connecticut Health Centre for providing us the transgenic *B. burgdorferi*, Bb914, and to Drs. Can Bruce, Albert Mennone Jr, and Amit Lahiri at Yale University for their advise on meta sequence

analysis, confocal microscopy and mobility shift assay respectively, and to Michael Schadt at the Histology Facility at Yale University, and Yasemin Ayetaman for excellent technical assistance. This work was supported by NIH grants to EF (AI32947, AI9200 and 41440). Erol Fikrig is an investigator of the Howard Hughes Medical Institute.

References

Agaisse H, Perrimon N. The roles of JAK/STAT signaling in *Drosophila* immune responses. Immunol Rev. 2004; 198:72–82. [PubMed: 15199955]

Aljamali MN, Sauer JR, Essenberg RC. RNA interference: applicability in tick research. Experimental & applied acarology. 2002; 28:89–96. [PubMed: 14570119]

Amcheslavsky A, Jiang J, Ip YT. Tissue damage-induced intestinal stem cell division in *Drosophila*. Cell Stem Cell. 2009; 4:49–61. [PubMed: 19128792]

Andreotti R, Perez de Leon AA, Dowd SE, Guerrero FD, Bendele KG, Scoles GA. Assessment of bacterial diversity in the cattle tick *Rhipicephalus (Boophilus) microplus* through tag-encoded pyrosequencing. BMC Microbiol. 2011; 11:6. [PubMed: 21211038]

Arbouzova NI, Zeidler MP. JAK/STAT signalling in *Drosophila*: insights into conserved regulatory and cellular functions. Development. 2006; 133:2605–2616. [PubMed: 16794031]

Barbour AG, Fish D. The biological and social phenomenon of Lyme disease. Science. 1993; 260:1610–1616. [PubMed: 8503006]

Beaty, BJ.; Marquardt, WC. The biology of disease vectors. Niwot, Colo: University Press of Colorado; 1996.

Boissiere A, Tchioffo MT, Bachar D, Abate L, Marie A, Nsango SE, Shahbazkia HR, Awono-Ambene PH, Levashina EA, Christen R, et al. Midgut microbiota of the malaria mosquito vector *Anopheles gambiae* and interactions with *Plasmodium falciparum* infection. PLoS Pathog. 2012; 8:e1002742. [PubMed: 22693451]

Broadwater AH, Sonenshine DE, Hynes WL, Ceraul S, De SA. Glass capillary tube feeding: a method for infecting nymphal *Ixodes scapularis* (Acari: Ixodidae) with the lyme disease spirochete *Borrelia burgdorferi*. J Med Entomol. 2002; 39:285–292. [PubMed: 11931028]

Broderick N, Lemaitre B. Gut-associated microbes of *Drosophila melanogaster*. Gut microbes. 2012; 3

Buchon N, Broderick NA, Chakrabarti S, Lemaitre B. Invasive and indigenous microbiota impact intestinal stem cell activity through multiple pathways in *Drosophila*. Genes & development. 2009a; 23:2333–2344. [PubMed: 19797770]

Buchon N, Broderick NA, Poidevin M, Pradervand S, Lemaitre B. *Drosophila* intestinal response to bacterial infection: activation of host defense and stem cell proliferation. Cell host & microbe. 2009b; 5:200–211. [PubMed: 19218090]

Cirimotich CM, Ramirez JL, Dimopoulos G. Native microbiota shape insect vector competence for human pathogens. Cell host & microbe. 2011; 10:307–310. [PubMed: 22018231]

Clemente JC, Ursell LK, Parfrey LW, Knight R. The impact of the gut microbiota on human health: an integrative view. Cell. 2012; 148:1258–1270. [PubMed: 22424233]

Das S, Banerjee G, DePonte K, Marcantonio N, Kantor FS, Fikrig E. Salp25D, an *Ixodes scapularis* antioxidant, is 1 of 14 immunodominant antigens in engorged tick salivary glands. The Journal of infectious diseases. 2001; 184:1056–1064. [PubMed: 11574922]

Devenport M, Alvarenga PH, Shao L, Fujioka H, Bianconi ML, Oliveira PL, Jacobs-Lorena M. Identification of the *Aedes aegypti* peritrophic matrix protein AeIMUCI as a heme-binding protein. Biochemistry. 2006; 45:9540–9549. [PubMed: 16878988]

Du XJ, Wang JX, Liu N, Zhao XF, Li FH, Xiang JH. Identification and molecular characterization of a peritrophin-like protein from fleshy prawn (*Fenneropenaeus chinensis*). Molecular immunology. 2006; 43:1633–1644. [PubMed: 16271393]

Dunham-Ems SM, Caimano MJ, Pal U, Wolgemuth CW, Eggers CH, Balic A, Radolf JD. Live imaging reveals a biphasic mode of dissemination of *Borrelia burgdorferi* within ticks. The Journal of clinical investigation. 2009; 119:3652–3665. [PubMed: 19920352]

Fire A, Xu S, Montgomery MK, Kostas SA, Driver SE, Mello CC. Potent and specific genetic interference by double-stranded RNA in *Caenorhabditis elegans*. Nature. 1998; 391:806–811. [PubMed: 9486653]

Goddard, J. Infectious diseases and arthropods. Totowa, N.J: Humana Press; 2000.

Gravitz L. Microbiome: The critters within. Nature. 2012; 485:S12–13. [PubMed: 22616099]

Grigor'eva LA, Amosova LI. Peritrophic matrix in the midgut of tick females of the genus *Ixodes* (Acari: Ixodidae). Parazitologiia. 2004; 38:3–11. [PubMed: 15069874]

Hegedus D, Erlandson M, Gillott C, Toprak U. New insights into peritrophic matrix synthesis, architecture, and function. Annu Rev Entomol. 2009; 54:285–302. [PubMed: 19067633]

Hladik, FLCaC. A Self-Instructional Text. 3. American Society for Clinical Pathology; 1997. Histotechnology.

Hong SH, Park SK, Cho YS, Lee HS, Kim KR, Kim MG, Chung WH. Gentamicin induced nitric oxide-related oxidative damages on vestibular afferents in the guinea pig. Hearing research. 2006; 211:46–53. [PubMed: 16289993]

Jeney V, Balla J, Yachie A, Varga Z, Vercellotti GM, Eaton JW, Balla G. Pro-oxidant and cytotoxic effects of circulating heme. Blood. 2002; 100:879–887. [PubMed: 12130498]

Jiang H, Patel PH, Kohlmaier A, Grenley MO, McEwen DG, Edgar BA. Cytokine/Jak/Stat signaling mediates regeneration and homeostasis in the *Drosophila* midgut. Cell. 2009; 137:1343–1355. [PubMed: 19563763]

Karsten P, Hader S, Zeidler MP. Cloning and expression of *Drosophila* SOCS36E and its potential regulation by the JAK/STAT pathway. Mech Dev. 2002; 117:343–346. [PubMed: 12204282]

Kopacek P, Hajdusek O, Buresova V, Daffre S. Tick innate immunity. Advances in experimental medicine and biology. 2010; 708:137–162. [PubMed: 21528697]

Kuraishi T, Binggeli O, Opota O, Buchon N, Lemaitre B. Genetic evidence for a protective role of the peritrophic matrix against intestinal bacterial infection in *Drosophila melanogaster*. Proceedings of the National Academy of Sciences of the United States of America. 2011; 108:15966–15971. [PubMed: 21896728]

Lehane MJ. Peritrophic matrix structure and function. Annu Rev Entomol. 1997; 42:525–550. [PubMed: 15012322]

Ley RE, Lozupone CA, Hamady M, Knight R, Gordon JI. Worlds within worlds: evolution of the vertebrate gut microbiota. Nat Rev Microbiol. 2008; 6:776–788. [PubMed: 18794915]

Liu L, Dai J, Zhao YO, Narasimhan S, Yang Y, Zhang L, Fikrig E. Ixodes scapularis JAK-STAT Pathway Regulates Tick Antimicrobial Peptides, Thereby Controlling the Agent of Human Granulocytic Anaplasmosis. The Journal of infectious diseases. 2012; 206:1233–1241. [PubMed: 22859824]

Liu X, Robinson GW, Gouilleux F, Groner B, Hennighausen L. Cloning and expression of Stat5 and an additional homologue (Stat5b) involved in prolactin signal transduction in mouse mammary tissue. Proceedings of the National Academy of Sciences of the United States of America. 1995; 92:8831–8835. [PubMed: 7568026]

Margulies M, Egholm M, Altman WE, Attiya S, Bader JS, Bemben LA, Berka J, Braverman MS, Chen YJ, Chen Z, et al. Genome sequencing in microfabricated high-density picolitre reactors. Nature. 2005; 437:376–380. [PubMed: 16056220]

Martin PA, Schmidtmann ET. Isolation of aerobic microbes from *Ixodes scapularis* (Acari: Ixodidae), the vector of Lyme disease in the eastern United States. J Econ Entomol. 1998; 91:864–868. [PubMed: 9725033]

Munderloh UG, Kurtti TJ. Cellular and molecular interrelationships between ticks and prokaryotic tick-borne pathogens. Annu Rev Entomol. 1995; 40:221–243. [PubMed: 7810987]

Narasimhan S, Sukumaran B, Bozdogan U, Thomas V, Liang X, DePonte K, Marcantonio N, Koski RA, Anderson JF, Kantor F, et al. A tick antioxidant facilitates the Lyme disease agent's successful migration from the mammalian host to the arthropod vector. Cell host & microbe. 2007; 2:7–18. [PubMed: 18005713]

Neelakanta G, Li X, Pal U, Liu X, Beck DS, DePonte K, Fish D, Kantor FS, Fikrig E. Outer surface protein B is critical for Borrelia burgdorferi adherence and survival within Ixodes ticks. PLoS Pathog. 2007; 3:e33. [PubMed: 17352535]

Ng KM, Ferreyra JA, Higginbottom SK, Lynch JB, Kashyap PC, Gopinath S, Naidu N, Choudhury B, Weimer BC, Monack DM, et al. Microbiota-liberated host sugars facilitate post-antibiotic expansion of enteric pathogens. Nature. 2013; 502:96–99. [PubMed: 23995682]

Osset J, Bartolome RM, Garcia E, Andreu A. Assessment of the capacity of Lactobacillus to inhibit the growth of uropathogens and block their adhesion to vaginal epithelial cells. The Journal of infectious diseases. 2001a; 183:485–491. [PubMed: 11133381]

Osset J, Garcia E, Bartolome RM, Andreu A. Role of *Lactobacillus* as protector against vaginal candidiasis. Medicina clinica. 2001b; 117:285–288. [PubMed: 11571120]

Pal U, Li X, Wang T, Montgomery RR, Ramamoorthi N, Desilva AM, Bao F, Yang X, Pypaert M, Pradhan D, et al. TROSPA, an *Ixodes scapularis* receptor for *Borrelia burgdorferi*. Cell. 2004; 119:457–468. [PubMed: 15537536]

Piuri M, Sanchez-Rivas C, Ruzal SM. A novel antimicrobial activity of a *Paenibacillus polymyxa* strain isolated from regional fermented sausages. Letters in applied microbiology. 1998; 27:9–13. [PubMed: 9722991]

Radolf JD, Caimano MJ, Stevenson B, Hu LT. Of ticks, mice and men: understanding the dual-host lifestyle of Lyme disease spirochaetes. Nat Rev Microbiol. 2012; 10:87–99. [PubMed: 22230951]

Rajan A, Perrimon N. *Drosophila* cytokine unpaired 2 regulates physiological homeostasis by remotely controlling insulin secretion. Cell. 2012; 151:123–137. [PubMed: 23021220]

Rani A, Sharma A, Rajagopal R, Adak T, Bhatnagar RK. Bacterial diversity analysis of larvae and adult midgut microflora using culture-dependent and culture-independent methods in lab-reared and field-collected *Anopheles stephensi*-an Asian malarial vector. BMC Microbiol. 2009; 9:96. [PubMed: 19450290]

Rivas ML, Cobreros L, Zeidler MP, Hombria JC. Plasticity of *Drosophila* Stat DNA binding shows an evolutionary basis for Stat transcription factor preferences. EMBO Rep. 2008; 9:1114–1120. [PubMed: 18802449]

Shao L, Devenport M, Fujioka H, Ghosh A, Jacobs-Lorena M. Identification and characterization of a novel peritrophic matrix protein, Ae-Aper50, and the microvillar membrane protein, AEG12, from the mosquito, Aedes aegypti. Insect Biochem Mol Biol. 2005; 35:947–959. [PubMed: 15978997]

Soares CA, Lima CM, Dolan MC, Piesman J, Beard CB, Zeidner NS. Capillary feeding of specific dsRNA induces silencing of the *isac* gene in nymphal *Ixodes scapularis* ticks. Insect Mol Biol. 2005; 14:443–452. [PubMed: 16033437]

Sojka D, Hajdusek O, Dvorak J, Sajid M, Franta Z, Schneider EL, Craik CS, Vancova M, Buresova V, Bogyo M, et al. IrAE: an asparaginyl endopeptidase (legumain) in the gut of the hard tick *Ixodes ricinus*. Int J Parasitol. 2007; 37:713–724. [PubMed: 17336985]

Spor A, Koren O, Ley R. Unravelling the effects of the environment and host genotype on the gut microbiome. Nat Rev Microbiol. 2011; 9:279–290. [PubMed: 21407244]

Steere AC, Malawista SE, Snydman DR, Shope RE, Andiman WA, Ross MR, Steele FM. Lyme arthritis: an epidemic of oligoarticular arthritis in children and adults in three connecticut communities. Arthritis Rheum. 1977; 20:7–17. [PubMed: 836338]

Thomas V, Anguita J, Barthold SW, Fikrig E. Coinfection with *Borrelia burgdorferi* and the agent of human granulocytic ehrlichiosis alters murine immune responses, pathogen burden, and severity of Lyme arthritis. Infection and immunity. 2001; 69:3359–3371. [PubMed: 11292759]

Wang Y, Gilbreath TM 3rd, Kukutla P, Yan G, Xu J. Dynamic gut microbiome across life history of the malaria mosquito *Anopheles gambiae* in Kenya. PloS one. 2011; 6:e24767. [PubMed: 21957459]

Weiss B, Aksoy S. Microbiome influences on insect host vector competence. Trends in parasitology. 2011; 27:514–522. [PubMed: 21697014]

Weiss BL, Wang J, Maltz MA, Wu Y, Aksoy S. Trypanosome infection establishment in the tsetse fly gut is influenced by microbiome-regulated host immune barriers. PLoS Pathog. 2013; 9:e1003318. [PubMed: 23637607]

Welchman DP, Aksoy S, Jiggins F, Lemaitre B. Insect immunity: from pattern recognition to symbiont-mediated host defense. Cell host & microbe. 2009; 6:107–114. [PubMed: 19683677]

Zeidler MP, Bach EA, Perrimon N. The roles of the *Drosophila* JAK/STAT pathway. Oncogene. 2000; 19:2598–2606. [PubMed: 10851058]

Zeidler MP, Bausek N. The *Drosophila* JAK-STAT pathway. Jak-Stat. 2013; 2:e25353. [PubMed: 24069564]

HIGHLIGHTS

- Tick gut microbiota modulate Lyme disease spirochete *B. burgdorferi* colonization
- Expression of the transcription factor STAT is decreased in dysbiosed tick larvae
- STAT regulates tick gut peritrophic membrane integrity via peritrophin expression
- Tick peritrophic membrane integrity is critical for spirochete colonization

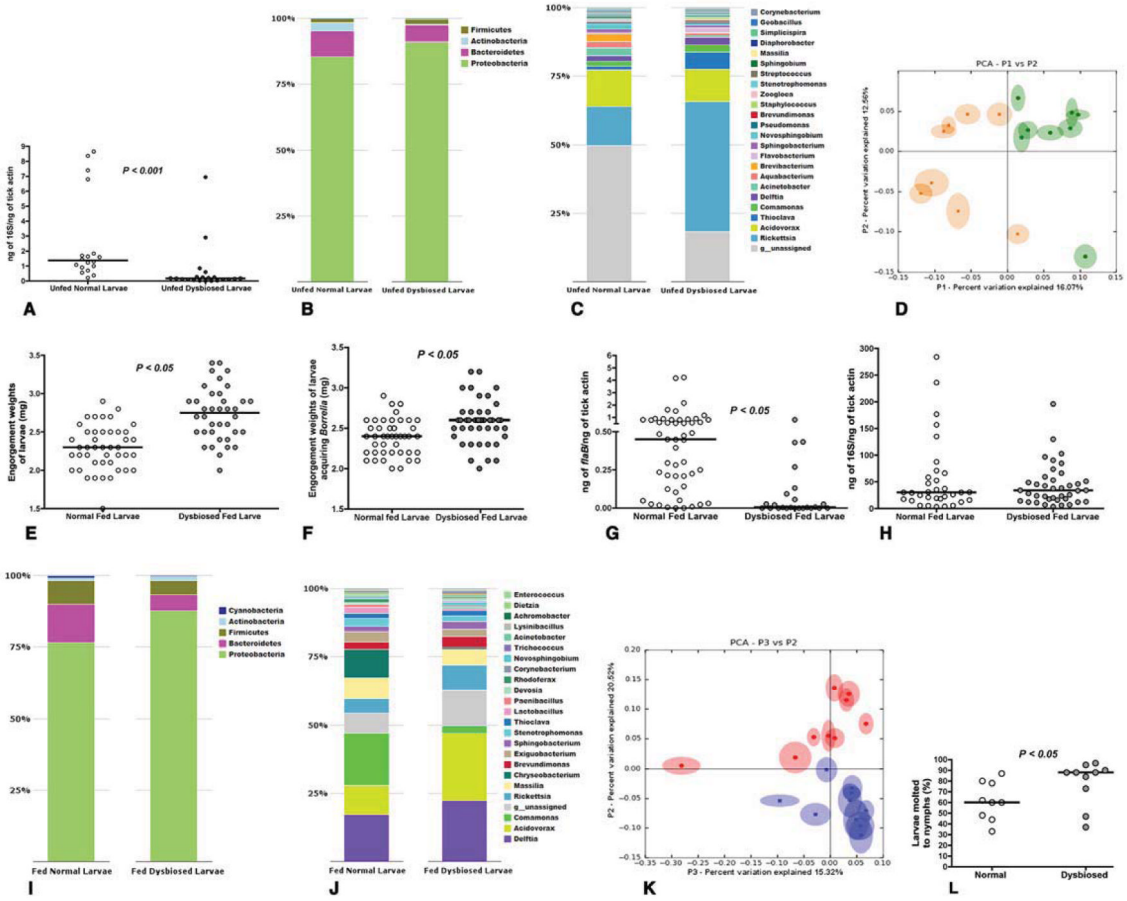

Figure 1. Dysbiosis alters larval feeding, and molting efficiency

A. Quantitative PCR (QPCR) of 16S rDNA in Unfed normal and unfed dysbiosed larvae. **B.** Phylum; and **C**. Genera level composition of unfed normal and dysbiosed larvae; **D**. Principal Coordinate Analysis of unweighted jack-knifed UniFrac distances of microbial communities from unfed normal (green) and unfed dysbiosed larvae (yellow). **E**. Engorgement weights of normal and dysbiosed larvae fed on clean C3H mice. **F**. Engorgement weights of normal and dysbiosed larvae fed on *B. burgdorferi*-infected C3H mice. **G**. QPCR analysis of *B. burgdorferi* burden in normal and dysbiosed larvae fed on *B. burgdorferi*-infected C3H mice. **H**. QPCR of 16S rDNA in fed normal and dysbiosed larvae. **I**. Phylum, and **J**. Genera level composition of fed normal and dysbiosed larvae. **K.** Principal Coordinate Analysis of unweighted jack-knifed UniFrac distances of microbial communities from fed normal (blue) and fed dysbiosed larvae (red). **L**. Molting efficiency of engorged normal and dysbiosed larvae assessed 8 weeks post feeding. Each data point represents a percentage of 50 larvae/tube. Each data point in A, D, and K represents ~ 20 larvae and E, F, G, and H represents pools of 5 larvae. Horizontal bars represent the median, and mean values significantly different in a two-tailed non-parametric Mann-Whitney test ($P < 0.05$) indicated. In B, C, I, and J all detectable components at the phylum level are shown, and up to 23 dominant components (> 0.05 %) at the family level are shown. See also Fig S1.

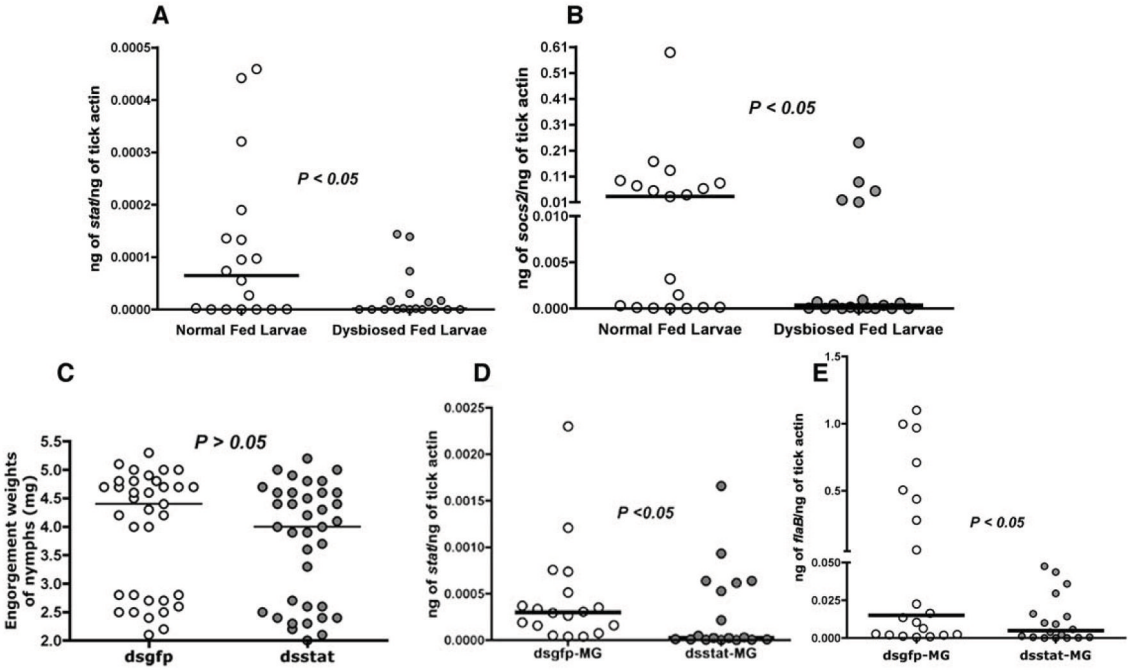

Figure 2. Expression of stat is decreased in dysbiosed larvae and RNA interference mediated knockdown of *stat* impairs *B. burgdorferi* colonization

Quantitative RT-PCR assessment of expression of *stat* (**A**) and *socs2* (**B**) in normal and dysbiosed larvae engorged on *B. burgdorferi*-infected C3H mice. Each data point represents a pool of 5 engorged larvae. **C**. Engorgement weights of dsstat, or dsgfp RNA injected nymphs fed on *B. burgdorferi*-infected C3H mice. Each data point represents 1 nymph. Quantitative-RT-PCR analysis of: **D**. Expression levels of *stat;* and **E**. *B. burgdorferi* burden in dsstat, or dsgfp RNA-injected nymphs fed to repletion on *B. burgdorferi*-infected C3H mice. Each data point in D–E represents a pool of 2–3 nymph guts. Horizontal bars represent the median and mean values significantly different in a two-tailed non-parametric Mann-Whitney test ($P < 0.05$) indicated.

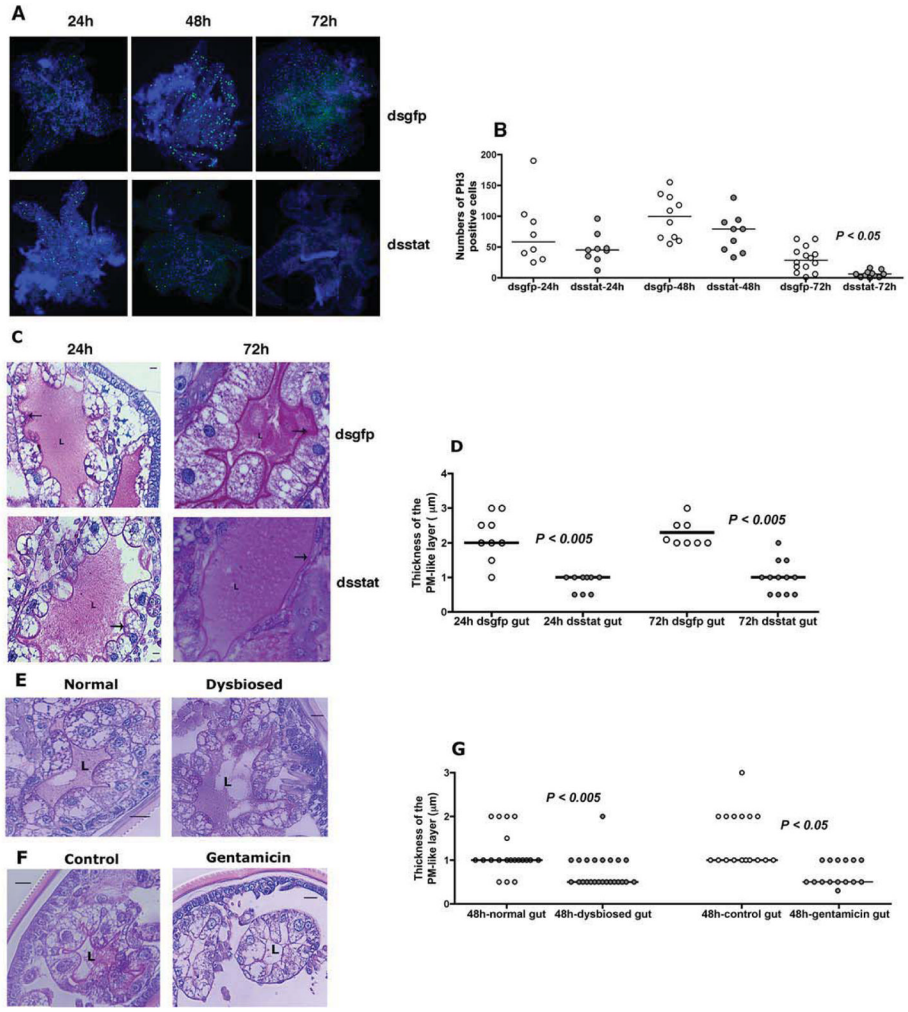

Figure 3. RNA interference-mediated knockdown of *stat* expression correlates with altered gut barrier integrity

A. Immunofluorescence microscopy to assess mitotic activity in nymhpal guts of dsgfp or dsstat RNA-injected nymphs at 24, 48, and 72 h of feeding as seen by PH3 positive signal (green/Alexa 488). Nuclei stained with DAPI (Blue). Magnification x10; and **B**. Quantitation of PH3 positive signal/gut. Each data point represents one gut. **C**. Periodic acid-Schiff's (PAS) stain of Carnoy's fixed and sectioned 24 and 72h fed guts of dsgfp or dsstat RNA-injected nymphal guts; and **D**. Thickness of the PM-like layer. PAS stain of Carnoy's fixed and sectioned 48 h fed guts of: **E**. Normal and dysbiosed larvae; and **F**. PBS or gentamicin-exposed larvae stained with PAS; and **G**. Thickness of the PM-like layer. 'L' indicates the lumen and arrow indicates the PM layer. In **C**, **E** and **F**, scale bars are 10 μm and magnification at 40x. In **D** and **G**, each data point represents an arithmetic average of 3 measurements/field/gut. Horizontal bars represent the median and mean values significantly different in a non-parametric two-tailed Mann-Whitney test ($P < 0.05$) indicated. See also Fig S2.

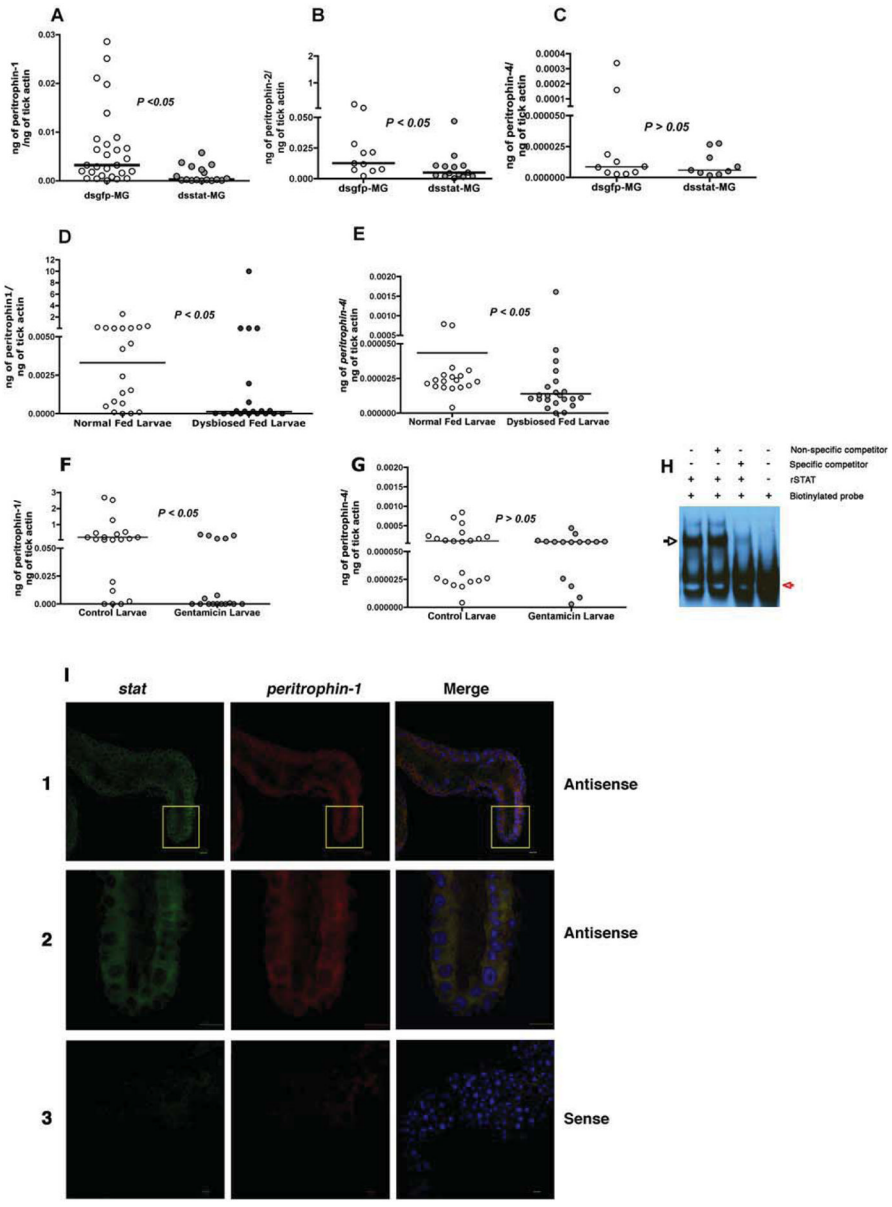

Figure 4. Dysbiosis alters the expression of *peritrophin-1* and 4

Quantitative-RT-PCR analysis of expression levels of *peritrophin-1, 2 and 4* in replete: guts of dsgfp and dsstat RNA-injected nymphs (**A–C**); normal and dysbiosed larvae (**D–E**); and PBS or gentamicin-exposed larvae **(F–G).** See also Figure S5. Horizontal bars represent the median and mean values significantly different in a two-tailed non-parametric Mann-Whitney test ($P < 0.05$) indicated. **H**. EMSA assessment of STAT binding to *peritrophin-1* promoter region. Recombinant STAT (rSTAT) incubated with biotinyated DNA (Biotinylated probe) alone or with unlabeled probe (Specific competitor) containing the conserved STAT-binding site of *peritrophin-1* or with unlabeled irrelevant probe (Non-specific competitor). Red and black arrows indicate biotinylated probe and electrophoretic mobility shift of the botinylated probe respectively. **I**. RNA-FISH shows co-expression of *stat* and *peritrophin-1* transcripts in gut epithelial cells. Fixed and permeabilized 48 h-fed tick guts stained with: Panel 1. Alexa488-labeled *stat* antisense RNA (green) and Alexa 555-labeled *peritrophin-1* antisense RNA (red); Panel 2. Alexa488-labeled *stat* sense RNA

(green) and Alexa 555-labeled *peritrophin-1* sense RNA (red). Nuclei stained with Topro-3 (blue). Panels 1 and 3 at 25x magnification. Panel 2 shows a portion of Panel 1 at 63x magnification. See also Fig S3.

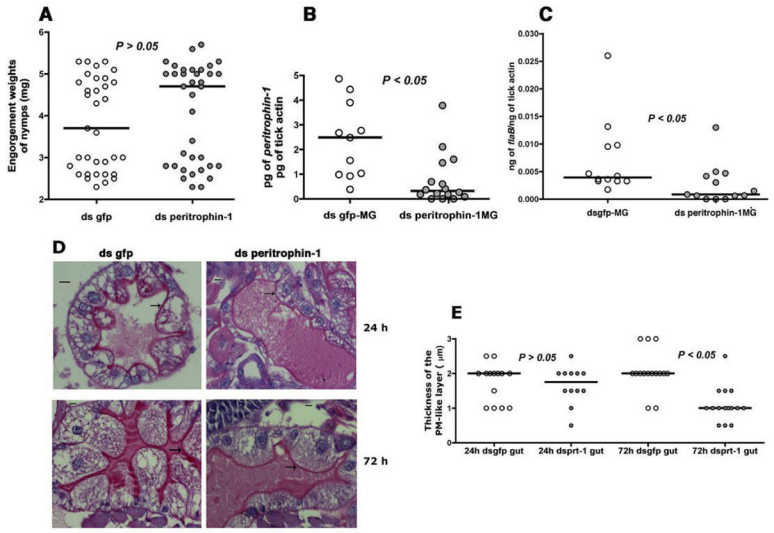

Figure 5. RNA interference-mediated knockdown of *peritrophin* expression alters the peritrophic matrix and impairs *B. burgdorferi* colonization

A. Engorgement weights; and **B**. Quantitative-RT-PCR assessment of expressions of *peritrophin-1*, and **C**. *flaB* in engorged ds gfp or ds peritrophin-1-injected nymphal guts fed on *B. burgdorferi*-infected C3H mice. Each data point in **A** represents 1 nymph, and in **B** and **C** represents a pool of 2–3 nymphal guts. **D**. Periodic acid-Schiff's (PAS) stain of Carnoy's fixed and sectioned 24, and 72h fed guts of dsgfp or ds*peritrophin-1* RNA-injected nymphal guts stained with stain. Magnification x40, scale bar, 10 μm. Arrows indicate the PAS-positive PM-like layer; and **E**. Thickness of the PM-like layer. Each data point represents an arithmetic average of 3 measurements/field/gut. Horizontal bars in **A**, **B**, **C** and **E** represent the median and mean values significantly different in a non-parametric two-tailed Mann-Whitney test ($P < 0.05$) indicated.

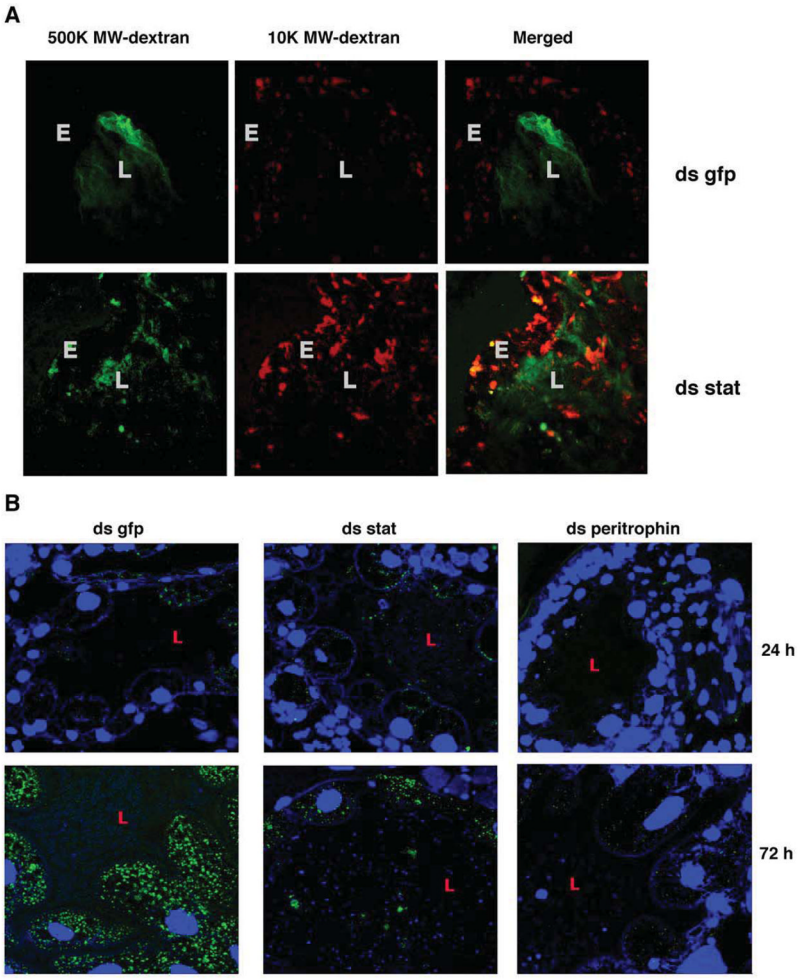

Figure 6. ***Borrelia burgdorferi*** **leaves the gut lumen and attaches to the gut epithelial cells during colonization**

Confocal microscopy of: **A**. 24 h fed guts of ds gfp or ds stat RNA-injected nymphs that were capillary-fed Rhodamine red-conjugated 10,000 molecular weight dextran (10 K MW dextran) and Fluorescein-conjugated 500,000 molecular weight dextran (500 K dextran). Magnification x40. 'L' marks the lumen and 'E' the gut epithelium. **B**. Carnoy's fixed and sectioned guts from dsgfp, dsstat, or dsperitrophin RNA-injected nymphs fed for 24 and 72 h on *B. burgdorferi*-infected C3H mice. Midgut nuclei and spirochetes stained with TO-PRO-3 (blue) and FITC-conjugated *B. burgdorferi* antisera (green), respectively. Magnification x63. 'L' marks the gut lumen.

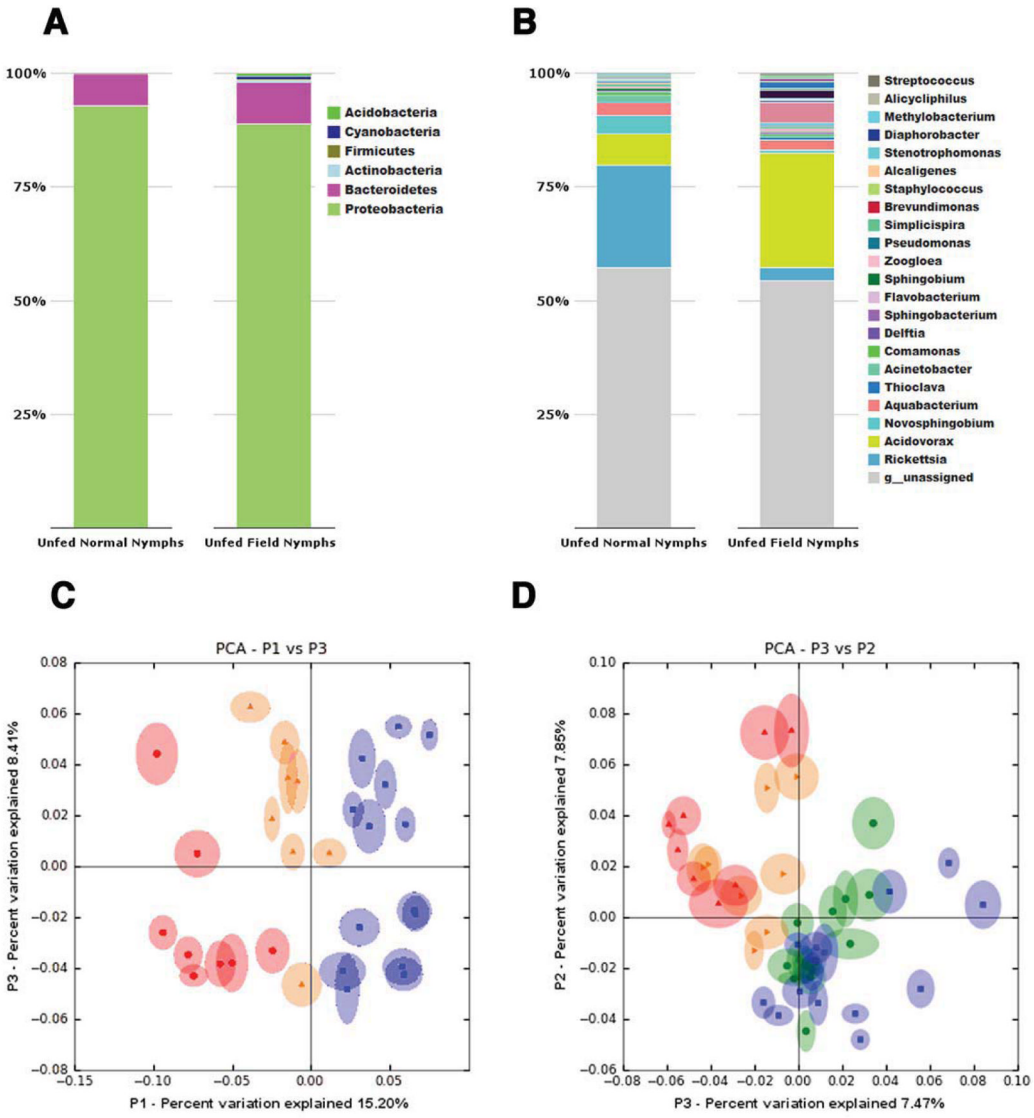

Figure 7. Comparison of the gut microbiota composition of laboratory-reared unfed larvae, nymphs and field-collected nymphs

A. Phylum, and **B**. Genera level composition of unfed lab-reared and field collected nymphs. Principle coordinate analysis of unweighted jack-knifed UniFrac distances of microbial communities from unfed: **C**. laboratory-reared normal larvae (yellow), dysbiosed larvae (red) and field-collected nymphs (blue); and **D**. laboratory-reared normal larvae (yellow), dysbiosed larvae (red), normal nymphs (green) and field-collected nymphs (blue). Each data point represents a pool of ~20 larvae, or individual nymphs.